A Two-Process Model Describes the Hydrogen Exchange Behavior of Cytochrome *c* in the Molten Globule State with Various Extents of Acetylation†

Zbigniew Szewczuk,‡,§ Yasuo Konishi,*,‡ and Yuji Goto*,||

Biotechnology Research Institute, National Research Council of Canada, 6100 Royalmount Avenue, Montreal, Quebec, Canada H4P 2R2, and Institute for Protein Research, Osaka University, 3-2 Yamadaoka, Suita, Osaka 565-0871, Japan

Received December 5, 2000; Revised Manuscript Received March 19, 2001

ABSTRACT: Acetylation of Lys residues of horse cytochrome *c* steadily stabilizes the molten globule state in 18 mM HCl as more Lys residues are acetylated [Goto and Nishikiori (1991) *J. Mol. Biol. 222*, 679−686]. The dynamic features of the molten globule state were characterized by hydrogen/deuterium exchange of amide protons, monitored by mass spectrometry as each deuteration increased the protein mass by 1 Da. Electrospray mass spectrometry enabled us to monitor simultaneously the exchange kinetics of more than seven species with a different number of acetyl groups. One to four Lys residue-acetylated cytochrome *c* showed almost no protection of the amide protons from rapid exchange. The transition from the unprotected to the protected state occurred between five and eight Lys residue-acetylated species. For species with more than nine acetylated Lys residues, the exchange kinetics were independent of the extent of acetylation, and 26 amide protons were protected at 60 min of exchange, indicating the formation of a rigid hydrophobic core with hydrogen-bonded secondary structures. The apparent transition to the protected state required a higher degree of acetylation than the conformational transition measured by circular dichroism, which had a midpoint at about four acetylated residues. This difference in the transitions suggested a two-process model in which the exchange occurs either from the protected folded state or from the unprotected unfolded state through global unfolding. On the basis of a two-process model and with the reported values of the exchange and stability parameters, we simulated the exchange kinetics of a series of acetylated cytochrome *c* species. The simulated kinetics reproduced the observed kinetics well, indicating validity of this model for hydrogen exchange of the molten globule state.

Hydrogen/deuterium (H/D)[1] exchange is one of the most important approaches to characterize protein dynamics. In combination with NMR, H/D exchange allows analysis of the dynamics of protein structure at the residue level (*1*−*6*). H/D exchange is powerful for characterizing the marginal conformational states that are often difficult to analyze directly and has been effectively used to elucidate the molecular structure of the intermediate states of protein folding (*7*−*11*). The kinetic (*8*) and equilibrium intermediates (*9*) of horse cytochrome *c* were the first examples of clarification of the molecular structures of folding intermediates by H/D exchange combined with NMR. Recent advances using ultrarapid mixing techniques enabled the characterization of the early intermediate accumulated at the submillisecond time regime (*12*).

On the other hand, mass spectroscopy (MS), measuring the changes in mass on H/D exchange, is also an important method for analyzing the H/D exchange reaction (*13*−*20*). While MS essentially provides the mass-to-charge ratio of a sample, more information can be extracted when electrospray MS is applied to proteins. For example, net charge of a protein molecule is sensitive to the protein conformation (*13*, *17*−*20*); i.e., disordered proteins have a large number of net charges, up to one charge for every 11 residues, whereas native proteins have fewer net charges, reflecting their compact structure. From the bimodal charge-state distribution of bovine cytochrome *c* at pH 2.7, Wagner and Anderegg (*17*) identified the coexistence of the native and disordered states in the same solution. Taking advantage of the simultaneous detection, they analyzed the H/D exchange reaction of the native and disordered states and obtained the same exchange kinetics, suggesting the rapid interconversion of the two states compared to the rate of H/D exchange. Thus, MS has the unique ability to characterize mixtures of different conformations or proteins without purification. However, MS does not have the structural resolution of NMR. Therefore, the two approaches are complementary: while NMR is useful to obtain high-resolution information at the residue level, MS is useful for separation of distinct

† This work is supported by the Japanese Ministry of Education, Science, Culture and Sports. NRCC Publication No. 44789.

* Corresponding authors. Y.G.: fax, +81 (6) 6879-8616; e-mail, ygoto@protein.osaka-u.ac.jp. Y.K.: fax, (514) 496-5143; e-mail, Yasuo.Konishi@nrc.ca.

‡ Biotechnology Research Institute, National Research Council of Canada.

§ Current address: Faculty of Chemistry, University of Wroclaw, ul. F. Joliot-Curie 14, 50-383 Wroclaw, Poland.

|| Institute for Protein Research, Osaka University.

[1] Abbreviations: ΔG_U, free energy change of unfolding; H/D, hydrogen/deuterium; MS, mass spectroscopy; *n*Ac-cyt *c*, modified cytochrome *c* with *n* Lys residues acetylated; NMR, nuclear magnetic resonance; P, protection factor; SAXS, small-angle X-ray scattering.

10.1021/bi002762c CCC: $20.00
Published on Web 07/17/2001

populations with respect to mass and for simultaneous analysis of a mixture of species.

We expected that analysis of the H/D exchange behavior of the molten globule state of horse cytochrome *c* (*21*−*23*) by MS would provide an important example of the H/D exchange kinetics of the intermediate state of protein folding. While cytochrome *c* is unfolded in the absence of salt at pH 2, the addition of salt stabilizes the molten globule state because the anion binding shields the charge repulsion between the positively charged amino groups, and consequently the intrinsic hydrophobic effects manifest themselves (*22*, *23*). The molecular structure of the salt-stabilized molten globule state of cytochrome *c* has been analyzed by H/D exchange combined with NMR, which demonstrated the presence of major helices and disordering of the rest of the molecule (*9*, *24*). Goto and co-workers analyzed the compactness and thermodynamic stability of the molten globule state using a series of acetylated cytochrome *c* species (*25*−*27*). They showed that the molten globule state can be stabilized by acetylation of amino groups because the acetylation decreases the unfavorable charge repulsion. Acetylation-induced folding of cytochrome *c* could be approximated well by a two-state transition mechanism between the unfolded state and the compact molten globule state.

To obtain further insight into the exchange behavior of the intermediate conformational state, we used electrospray MS to measure the H/D exchange kinetics of cytochrome *c* with various degrees of acetylation. Electrospray mass spectrometry enabled us to monitor simultaneously the exchange kinetics of more than 10 species. While the intact cytochrome *c* in the absence of salt at pH 2 was easily exchanged in 10 min, the acetylation of amino groups progressively retarded the exchange reaction, representing the formation of the molten globule state protected from rapid exchange. However, the transition to the protected state measured by H/D exchange required a higher degree of acetylation than the apparent conformational transitions measured by CD and other methods. On the basis of a two-process model in which H/D exchange occurs either directly from the folded state or through the unfolded state, the kinetics of a series of acetylated species were satisfactorily reproduced with the reported values of the free energy change of unfolding (ΔG_U) (*26*), protection factors (*P*) of the salt-stabilized molten globule state (*9*), and the intrinsic exchange rate (k_{int}) (*28*).

EXPERIMENTAL PROCEDURES

Materials. Horse cytochrome *c*, acetic anhydride, and deuterium oxide (99.9 atom % D) were obtained from Sigma (St. Louis, MO) and were used without further purification. Deuterium chloride (20 wt % in D_2O) was from MSD Isotopes (Montreal, Quebec, Canada). Sodium acetate and ammonium acetate were purchased from Aldrich (Milwaukee, WI). Cytochrome *c* was acetylated by adding a 3.5- or 35-fold molar excess of acetic anhydride to 0.2 mL of cytochrome *c* solution (20 mg/mL) in 1 M sodium acetate. The reaction was carried out for 2 h at 0 °C. The byproduct *O*-acetyltyrosine residue is unstable under these conditions and regenerates Tyr residue (*29*). The products were desalted on a Sephadex G10 column (1.5 × 20 cm; equilibrated with 1% acetic acid; flow rate 3 mL/min with 1% acetic acid) prior to lyophilization. Since the N-terminal residue of cytochrome *c* is blocked by acetylation, only Lys residues were acetylated in this reaction. The numbers of acetylated Lys residues were determined with an API III electrospray mass spectrometer (Sciex, Concord, Ontario, Canada). The modified proteins are designated as *n*Ac-cyt *c*, where *n* reflects the number of acetylated Lys residues; e.g., 5Ac-cyt *c* is a cytochrome *c* derivative in which five Lys residues were acetylated. The sites of acetylation were not identified. Each species with different degrees of acetylation probably consisted of various species acetylated at different sites.

Electrospray Mass Spectra. The API III mass spectrometer in positive ion mode was used to monitor the deuteration kinetics. The ion spray needle was maintained at 5200 V, and the orifice potential was set at 100 V. The sample solution was infused continuously using a syringe pump (Model 22, Harvard Apparatus, South Natick, MA) with a flow rate of 1 μL/min. The molecular mass was determined with the first quadrupole, which was calibrated with the ammonium adduct ions of poly(propylene glycols). The molecular mass of the proteins was independent of the charge state and thus calculated by averaging the molecular masses of the peaks at various charge states. All experiments were performed at room temperature (∼20 °C). Since each acetylation increased the mass of the proteins by 42.04 Da, the peaks of *n*Ac-cyt *c* ($n = 0-13$) were well separated from each other, and electrospray MS could be applied to a mixture of *n*Ac-cyt *c* ($n = 1-6$ or $6-13$).

Deuteration of nAc-cyt c. The labile protons in proteins are the backbone amide protons and the side chain protons of some amino acids. In addition, the heme group has two exchangeable protons. However, since hydrogen exchange of the labile protons in the amino acid side chains is too fast to be monitored by MS, we studied only the backbone amide protons. Cytochrome *c* consists of 104 amino acids residues, containing 3 prolines, and the N-terminal is acetylated. Thus, there are 99 amide protons. A total of 0.1 mg of *n*Ac-cyt *c* ($n = 0$, $1-6$, or $6-13$) mixture was dissolved in 0.01 mL of 18 mM HCl (pH 1.8). The protein conformations were equilibrated by incubation for 30 min at room temperature. Deuteration was initiated at room temperature by adding 0.09 mL of 18 mM DCl/D_2O. The deuteration kinetics were monitored using the API III mass spectrometer. The kinetic data obtained were reliable because the mixture of *n*Ac-cyt *c* ($n = 0$, $1-6$, or $6-13$) was deuterated not only under the same solvent conditions but also in the same solution. All peaks were resolved during the deuteration experiments. The ionization chamber was enclosed and continually flushed with ultrapure nitrogen (Air Products and Chemicals, Inc., Allentown, PA; <2.0 ppm of H_2O content) to minimize the back-exchange of labile deuterium atoms in the proteins with hydrogen of water vapor of the ambient laboratory atmosphere (*14*). Only a residual amount of back-exchange (3.5 ± 1%) was observed. A range of mass-to-charge ratio (*m*/*z*) 700−2000 was scanned with a step size of 0.25. Several scans were averaged to improve the signal-to-noise ratio. The mass spectra were measured continuously for 45 min and then after 1, 2, and 24 h. As the extent of exchange is proportional to the D_2O concentration (*30*), the number of unexchanged protons *H*(r) in *n*Ac-cyt *c* ($n = 0-13$) was calculated as

$$H(\mathrm{r}) = (12360.1 + 42.04n - M_{\mathrm{obs}})/0.906 + (195 - n) \quad (1)$$

The average molecular mass of cytochrome *c* is 12360.1 Da, (42.04*n*) Da is the mass increase by acetylating *n* Lys residues, M_{obs} is the observed molecular mass of the protein at a given deuteration time, 0.906 Da is the mass increase when a proton is completely exchanged in the solvent of 90% D_2O/H_2O, and (195 − *n*) is the total number of exchangeable protons in *n*Ac-cyt *c*, including the side chain protons.

RESULTS

MS of Acetylated Cytochrome c. Acetic anhydride is widely used to neutralize the amino groups of proteins. Heterogeneous protein molecules, in which 1−6 or 6−13 Lys residues per molecule were acetylated, were obtained with a 3.5- or 35-fold molar excess of acetic anhydride, respectively. Mass spectra of mixtures of *n*Ac-cyt *c* (n = 1−6 and 6−13) in 18 mM HCl (pH 1.8) are shown in panels A and B of Figure 1, respectively. The peaks derived from various *n*Ac-cyt *c* (n = 0−13) were well separated due to the mass increase of 42.04 Da per acetylation (Figure 2). In fact, we could separate more than 10 species and, as will be described below, could follow their exchange kinetics simultaneously. The number of acetyl groups introduced was determined from the molecular masses of the proteins (Table 1).

The charge distribution of the acetylated proteins showed two clusters of peaks: one around 850−1100 *m*/*z* with abundant peaks at z = 12+ to 14+ and another around 1550−1650 *m*/*z* with an abundant peak at z = 8+ (Figure 1). It should be noted that, although *n* Lys residues were neutralized in *n*Ac-cyt *c*, the charge states of these abundant peaks were insensitive to the number of remaining basic residues (Table 1). A similar phenomenon was reported in acetylated ribonuclease A (*31*). The former cluster around 850−1100 *m*/*z* is commonly observed in disordered small proteins such as acid-denatured bovine cytochrome *c* (*17*) or acid-denatured horse apomyoglobin (*18*). In the case of bovine cytochrome *c*, the native state at neutral pH and the acid-denatured state at pH 2.5 have a maximum at z = 9+ and z = 16+, respectively, and a mixture of the two states at pH 2.7 showed the bimodal distribution with maxima at z = +9 and +15. Since *n*Ac-cyt *c* (n = 0−13) assumes either a disordered or a molten globule conformation at pH 1.8 (*25*−*27*), the later cluster around 1550−1650 *m*/*z* must come from the molten globule state. On the other hand, Wang and Tang (*18*) measured electrospray MS of acid-denatured horse apomyoglobin at pH 2 in the presence of various concentrations of ammonium trichloroacetate, a salt stabilizing the molten globule state, and observed the charge reduction with an increase in the concentration of salt. They suggested that the charge reduction is likely due to strong charge neutralization caused by the trichloroacetate anions, rather than to conformational changes of the protein. The present results with various acetylated cytochrome *c* species carried out in the same solution suggest that the formation of the compact molten globule state results in the charge reduction.

Native *n*Ac-cyt *c* (n = 0−13) at neutral pH also showed the most abundant peak at z = 8+ (data not shown). As the compactness of the molten globule is similar to that of the native conformation (*27*), the protein size seems to be the determinant of the most abundant charge state at z = 8+ (*17*). Interestingly, even highly acetylated 13Ac-cyt c, which is fully in the molten globule state in 18 mM HCl, showed strong peaks of disordered conformation (Figure 1B), whereas native *n*Ac-cyt *c* (n = 0−13) in neutral pH showed no trace of peaks of disordered conformation (data not

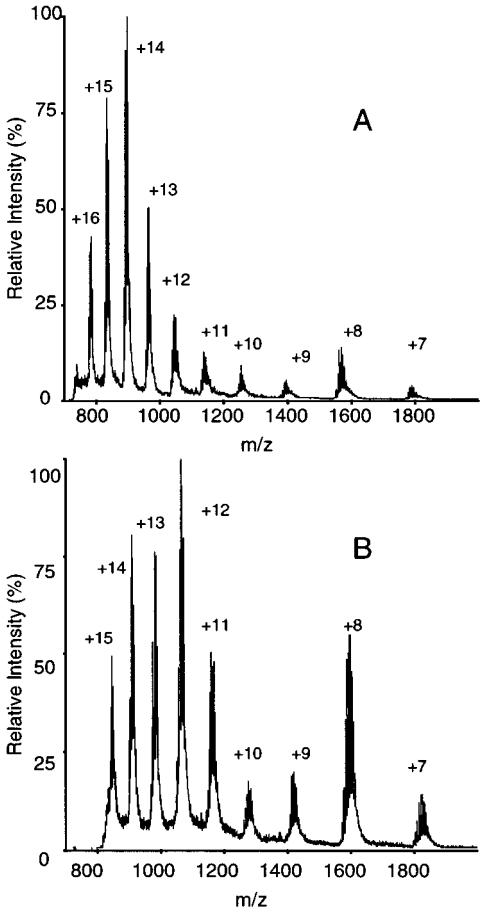

FIGURE 1: Mass spectra of a mixture of acetylated cytochrome *c* in 18 mM HCl (pH 1.8): (A) *n*Ac-cyt *c* (n = 1−6); (B) *n*Ac-cyt *c* (n = 6−13). The total concentration of the protein mixture was ∼4 mg/mL. Panels A and B show the accumulated spectra of 13 and 26 scans, respectively, with 0.1 *m*/*z* scan step and 1 ms dwell time.

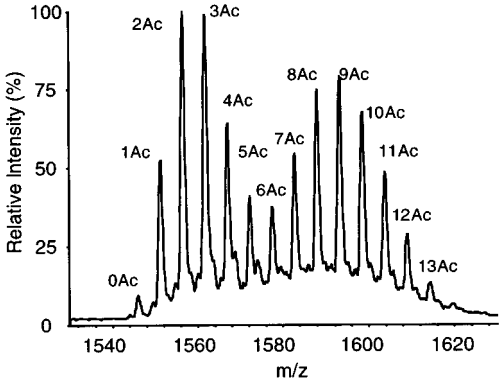

FIGURE 2: Mass spectrum of *n*Ac-cyt *c* (n = 0−13) in 18 mM HCl (pH 1.8). The peaks of 8+ net charged molecules are shown in the figure. The total concentration of the protein mixture was ∼8 mg/mL. The figure is the accumulated spectrum of 43 scans with 0.1 *m*/*z* scan step and 5 ms dwell time.

Table 1: Identification of Acetylated Cytochrome *c* by Mass Spectrometry

acetylated cytochrome *c*	MM_{calc} (Da)[a]	MM_{obs} (Da)[a]	*z* of abundant peak at	
			low *m*/*z*	high *m*/*z*
0Ac-cyt *c*	12 360.1	12 360.1 ± 2.0[b]	15+	8+
1Ac-cyt *c*	12 402.1	12 402.6 ± 1.2[b]	15+	8+
2Ac-cyt *c*	12 444.2	12 443.8 ± 1.2[b]	14+	8+
3Ac-cyt *c*	12 486.2	12 486.0 ± 0.8[b]	14+	8+
4Ac-cyt *c*	12 528.3	12 527.9 ± 1.0[b]	14+	8+
5Ac-cyt *c*	12 570.3	12 569.9 ± 1.0[b]	14+	8+
6Ac-cyt *c*	12 612.3	12 612.4 ± 2.1[b]	14+	8+
		12 612.6 ± 1.0[c]	14+	8+
7Ac-cyt *c*	12 654.4	12 655.2 ± 0.7[c]	14+	8+
8Ac-cyt *c*	12 696.4	12 696.9 ± 0.7[c]	14+	8+
9Ac-cyt *c*	12 738.5	12 739.0 ± 0.9[c]	14+	8+
10Ac-cyt *c*	12 780.5	12 781.1 ± 0.4[c]	12+	8+
11Ac-cyt *c*	12 822.5	12 822.8 ± 1.1[c]	12+	8+
12Ac-cyt *c*	12 864.6	12 864.8 ± 1.0[c]	12+	8+
13Ac-cyt *c*	12 906.6	12 907.3 ± 0.9[c]	12+	8+

[a] Calculated and observed average molecular masses. [b] Observed molecular masses of *n*Ac-cyt *c* ($n = 1-6$) mixture in 18 mM HCl. Deviations are standard deviations of molecular mass determined from all multiply charged peaks (Figure 1A). [c] Observed molecular masses of *n*Ac-cyt *c* ($n = 6 \pm 13$) mixture in 18 mM HCl. Deviations are standard deviations of molecular mass determined from all multiply charged peaks (Figure 1B).

shown) (*26*). This implied that the molten globule of *n*Ac-cyt *c* ($n = 0-13$) may not be stable in electrospray ionization. A higher population of the unfolded state observed in the mass spectrum than that in solution was also reported for bovine cytochrome *c* at pH 2.5 (*17*) and apomyoglobin at pH 7 (*18*). Thus, the denaturation in electrospray ionization may be common to the marginal conformational states, and inferences from the charge states of the ions to the solution structures of the proteins should be made cautiously.

H/D Exchange Kinetics. Deuteration of a protein may be initiated in two ways. One is to dissolve the protein in undeuterated solvent and to allow conformational equilibrium before diluting with deuterated solvent (*16*). This method requires a high protein concentration before dilution, and some amount of undeuterated solvent remains in the deuteration experiments. The other method is to dissolve a lyophilized sample directly into deuterated solvent to initiate the hydrogen−deuterium exchange reaction (*17*, *24*, *32*). The lyophilized protein is assumed to retain the solution conformation or to adopt the solution conformation in a very short time. This method allows deuteration in essentially 100% deuterated solvent. The two methods sometimes yield different results; e.g., the latter method showed the presence of at least two species of apomyoglobin with different deuteration rates, whereas the former method showed a single deuteration rate (*33*). We examined both methods and obtained comparable results; however, to avoid the uncertainty of the conformation of the lyophilized *n*Ac-cyt *c* ($n = 0-13$), we report here only the results obtained with the former method. Another advantage of the former method is that deuteration is initiated simultaneously for all molecules, whereas in the latter method it is necessary to dissolve a dried sample which may cause heterogeneity in the deuteration kinetics. The effect of deuteration on the stability of the protein conformations is another factor that must be addressed. Goto et al. (*34*) reported negligible effect of the deuterated solvent on the conformational stability of the molten globule state of *n*Ac-cyt *c* ($n = 0-13$).

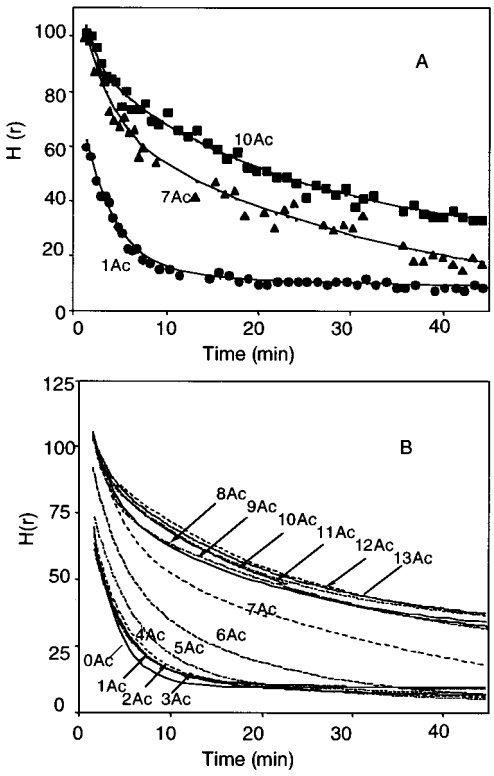

FIGURE 3: Deuteration kinetics of *n*Ac-cyt *c* ($n = 0-13$). (A) The data of 1Ac-cyt *c* (●), 7Ac-cyt *c* (▲), and 10Ac-cyt *c* (■) are plotted as examples. The deuteration kinetics of the proteins were fitted with eq 2, and the fitted curves are shown as solid lines. (B) Deuteration kinetics of *n*Ac-cyt *c* ($n = 0-13$). The fitted curves for all *n*Ac-cyt *c* ($n = 0-13$) are shown. *n*Ac-cyt *c* ($n = 0$, 1−6, or 6−13) was dissolved in 18 mM HCl (pH 1.8) at the total protein concentration of 10 mg/mL. Deuteration was initiated by diluting the proteins 10-fold with 18 mM DCl/D_2O. The number of exchangeable hydrogens *H*(r) remaining in the proteins was estimated from eq 1.

A mixture of *n*Ac-cyt *c* ($n = 0$, 1−6, or 6−13) was dissolved in 18 mM HCl (pH 1.8). After 30 min of incubation, deuteration was started by 10-fold dilution with 18 mM DCl/D_2O. No discrepancies were observed in the molecular masses estimated from the peaks of the disordered conformation and the molten globule state, indicating a rapid equilibrium between the two conformations compared to the deuteration rate, which is minimal around pH 3. A similar result was reported for bovine cytochrome *c* at pH 2.7, where the solution contains a mixture of the native and unfolded states (*17*). Thus, all peaks were used in determining the molecular masses of the proteins. As sharp peaks were observed throughout deuteration, the chemical heterogeneity of the acetylated Lys residues had little if any effect on the conformation and stability of the molten globule. The numbers of remaining amide protons in some *n*Ac-cyt *c* ($n = 0-13$) are plotted in Figure 3. Since hydrogen exchange of the labile protons in the amino acid side chains is too fast to be monitored by MS, it was expected that only the backbone amide protons could be detected. Cytochrome *c* consists of 104 amino acids residues, containing 3 prolines, and the N-terminal is acetylated. Thus, there are 99 amide protons. The observed kinetics showed the exchange behavior of about 100 protons, consistent with this expectation.

Although the overall exchange kinetics were likely to consist of multiple exponential terms, the data were ap-

proximated by fitting to an equation with two exponential terms:

$$H(\mathrm{r}) = H_1 \exp(-k_1 \mathrm{t}) + H_2 \exp(-k_2 \mathrm{t}) + H_3 \qquad (2)$$

H_1 represents the protons deuterated with a fast kinetic constant k_1, H_2 represents the protons deuterated with a slower kinetic constant k_2, and H_3 represents the protons fully protected from deuteration within 45 min and the back-exchanged hydrogen (3.5 ± 1%). The fitted curves for all *n*Ac-cyt *c* ($n = 0-13$) are shown in Figure 3B.

The deuteration of *n*Ac-cyt *c* ($n = 0-4$) occurred within 20 min and was essentially identical within experimental errors. The H_3 values of about 5 at 45 min probably came from the back-exchange during the measurements. Weak protection was then observed in 5Ac-cyt *c* for 20 min or less. 6Ac-cyt *c* protected more protons for 35 min or less. 7Ac-cyt *c* protected more protons for longer periods, and some protons were protected even after 1 h. Thus, above a certain level of stability, molten globules in the acetylated cytochrome *c* were able to protect amide protons from rapid deuteration. The protection was then saturated at 8Ac-cyt *c*. The deuteration kinetics of *n*Ac-cyt *c* ($n = 8-13$) were essentially the same up to 1 h, and 26 ± 1 protons were protected at 1 h, indicating the formation of a molten globule. The deuteration of *n*Ac-cyt *c* ($n = 8-10$) was completed within 1 day, whereas 7−13 protons of *n*Ac-cyt *c* ($n = 11-13$) were still protected after 1 day, suggesting formation of a core structure in *n*Ac-cyt *c* ($n = \sim 11-13$) (data not shown).

The acetylation-induced stabilization of the molten globule state of cytochrome *c* was previously analyzed by CD (*25*, *26*), SAXS, and tryptophan fluorescence (*27*). The acetylation-induced transition could be approximated well by a cooperative two-state mechanism (*25*−*27*, *34*). To compare the H/D exchange kinetics with those measured by other methods, we estimated the apparent time constant of the H/D exchange, a time that the number of remaining protected protons becomes 36 (=99/e). When estimating the apparent time constant, we subtracted the contributions of five unexchangeable protons observed even for 0Ac-cyt *c*. While it was 2.8 min for 0−3Ac-cyt *c*, it increased to 28 min for 12−13Ac-cyt *c*. Then, we plotted the normalized transition measured by the apparent time constant of exchange (Figure 4).

The difference between the transition measured by H/D exchange and that by CD was evident. The transitions measured by CD, SAXS, or tryptophan fluorescence agreed each other, consistent with a two-state transition mechanism: the midpoint of the transition was at 3−4Ac-cyt *c*, and the transition ended at about 10Ac-cyt *c*. In contrast, 1−4Ac-cyt *c* showed almost no change in the time constant of H/D exchange. The transition from the unprotected to the protected state occurred drastically between 5Ac-cyt *c* and 8Ac-cyt *c* species. Thus, the transition to the protected state measured by the time constant of exchange required a higher degree of acetylation than the apparent conformational transitions. The retardation of the H/D exchange monitored by electrospray MS was previously reported for the salt-stabilized molten globule state of horse apomyoglobin at pH 2 (*18*).

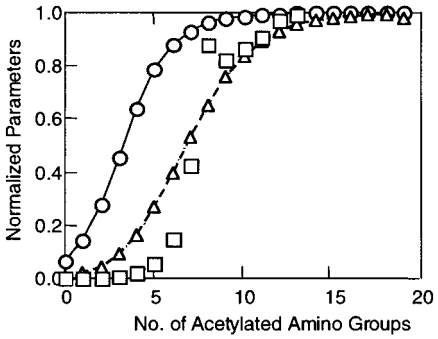

FIGURE 4: Normalized transitions of cytochrome *c* dependent on the degree of acetylation measured by CD at 222 nm (○) and observed (□) and calculated (△) overall time constants of hydrogen exchange at pH 2. The CD transition curve is a theoretical curve calculated with eq 7 and the parameters described in the text. The minimal and maximal values of the observed time constants of exchange were 2.8 and 27.8 min, respectively. Those of the calculated time constants were 3.5 and 13.8 min, respectively. For estimating the observed time constant, the contributions of five unexchanged protons were subtracted from the experimental kinetics.

DISCUSSION

In the present study, the effects of acetylation on protein conformation were analyzed by H/D exchange monitored by electrospray MS. We showed that the H/D exchange kinetics were significantly retarded with the progression of acetylation. However, the transition to the protected state required a higher degree of acetylation than the apparent conformational transitions (Figure 4). For species with extensive acetylation (i.e., more than nine acetylated Lys residues), the exchange kinetics were independent of the degree of acetylation, indicating formation of a stable molten globule state. We consider these observations in relation to the mechanism of H/D exchange.

Mechanism of H/D Exchange. Site-specific analysis with NMR has improved our understanding of the mechanism of H/D exchange. Among several mechanisms to explain the exchange reactions, the most generally accepted are EX1 and EX2 mechanisms on the basis of a common scheme (*5*, *6*, *35*):

$$\mathrm{NH(closed)} \underset{k_2}{\overset{k_1}{\rightleftharpoons}} \mathrm{NH(open)} \xrightarrow{k_{\mathrm{int}}} \mathrm{ND(open)} \qquad (3)$$

where the closed form, NH(closed), is in equilibrium with the open form, NH(open), with interconversion rate constants k_1 and k_2, and k_{int} is the intrinsic rate constant of exchange from the open form. In the EX2 mechanism, where the rates of conformational equilibrium (k_1 and k_2) are much faster than k_{int}, the observed exchange rate, k_{obs}, is described by $k_{\mathrm{obs}} = (k_1/k_2)k_{\mathrm{int}}$. In the EX1 mechanism, where the exchange is rate-limited by exposure of the amide protons, $k_{\mathrm{obs}} = k_1$. NMR has enabled the analysis at each amide site.

On the other hand, when the solution contains both the folded (F) and unfolded species (U), we have to consider a mechanism in which the exchange occurs either from the folded or unfolded states at each amide site (*5*, *36*).

$$\begin{array}{ccc} & \overset{k_{ex,F}}{\rightarrow} & \\ \mathrm{FH} & & \mathrm{FD} \\ k_F \uparrow\downarrow & & k_U \\ \mathrm{UH} & \underset{k_{ex,U}}{\rightarrow} & \mathrm{UD} \end{array} \qquad (4)$$

While many residues in the folded state are protected from exchange, the residues in the unfolded state are easily accessible to exchange. The exchange reaction of FH through UH to UD is similar to the reaction of eq 3, although eq 3 does not specify the conformation of the exchangeable state. The exchange rates between FH and UH, i.e., k_F and k_U, are probably much faster than $k_{ex,F}$ and $k_{ex,U}$ under the present experimental conditions at pH 2, where the intrinsic exchange rate is close to minimum. If this is a case, the process of conformational transition is approximated by an unfolding equilibrium constant, K_U ($=k_U/k_F$). Then, the apparent rate constant of the exchange reaction, k_{obs}, is represented by

$$k_{obs} = k_{ex,F}/(1 + K_U) + k_{ex,U}K_U/(1 + K_U) = k_{ex,F}f(F) + k_{ex,U}f(U) \quad (5)$$

where f(F) and f(U) are the fractions of the folded and unfolded states, respectively.

Under the conditions where the folded state is very stable, i.e., $K_U \ll 1$, eq 5 is approximated by

$$k_{obs} = k_{ex,F} + k_{ex,U}K_U \quad (6)$$

This is equivalent to the exchange rate of the two-process model with EX2 approximation for global unfolding (*5*, *6*). It is also noted that under the unfolding conditions, i.e., $K_U \gg 1$, eq 5 is simply k_{ex}, and at the midpoint of conformational transition where $K_U = 1$, $k_{obs} = (k_{ex,F} + k_{ex,U})/2$. Equation 5 is also useful for the unprotected amide protons in the folded state: If $k_{ex,F} = k_{ex,U}$, $k_{obs} = k_{ex,U}$. Thus, eq 5 can be considered to be a general form of a two-process model at each amide site, useful for describing the exchange behavior of various protons of different protection and under different conditions of protein stability. The only required assumption is that the approximation of k_F, $k_U \gg k_{ex,F}$, $k_{ex,U}$ holds. In the two-process model, the exchange of the protected amide protons in the folded state with a rate constant $k_{ex,F}$ has been proposed for two limiting cases, solvent penetration involving numerous small fluctuations and a discrete open/close transition involving specific local units (*5*, *6*). The exchange from the unfolded state often occurs at a rate similar to the intrinsic exchange rate ($k_{ex,U} \approx k_{int}$). These will be also valid for mechanism 4.

A two-process model has been used to explain the H/D exchange behavior of bovine pancreatic trypsin inhibitor (*37*), bovine ribonuclease A (*4*, *38*, *39*), and horse cytochrome *c* (*40*−*42*). Careful analysis of the H/D exchange of cytochrome *c* in the presence of low concentrations of denaturant revealed that the two-process model can be applied to several cooperative structural units, and a sequence of intermediate structures representing the pathway of unfolding has been proposed (*6*, *41*, *42*). Although these studies suggested that the two-process model is useful to analyze exchange from a partially folded state, to the best of our knowledge, no direct examples in which the two-process model held true for the exchange behavior of an isolated intermediate state have yet been reported. Therefore, it is intriguing if mechanism 4 and eq 5 can explain the H/D exchange behavior of the molten globule states of cytochrome *c* with various stabilities.

Equation 5, valid under different conditions of protein stability, indicates that, when the protein solution is a mixture of the folded and unfolded states, the apparent exchange behavior is biased by the labile unfolded state: when $k_{ex,F} \ll k_{ex,U}$, the time constant of the exchange reaction $(k_{obs})^{-1}$ is approximated by $(f(U)k_{ex,U})^{-1}$. In other words, it is not surprising that the transition to the protected state measured by the time constant of exchange required a higher degree of acetylation than the apparent conformational transitions.

Simulation of Exchange Kinetics. Thermodynamics of the acetylation-induced conformational transition of cytochrome *c* has been characterized in detail (*26*). In addition, protection factors (P) of the molten globule state of cytochrome *c* have been reported (*9*, *24*). Therefore, solely with the reported parameters, it will be possible to simulate the exchange kinetics on the basis of the general two-process model (mechanism 4 and eq 5). To obtain k_{obs} with eq 5, ΔG_U between the molten globule and unfolded states that provides f(F), and the exchange rates for the molten globule ($k_{ex,F}$) and the unfolded states ($k_{ex,U}$) are required.

(i) The Free Energy Change, ΔG_U. Hagihara et al. (*26*) analyzed the conformational stability of cytochrome *c* with various degrees of acetylation by CD and calorimetry and proposed an equation relating the net charge and ΔG_U at pH 2 and 20 °C:

$$\Delta G_U = \Delta G_U(\text{neutral}) + pZ^2 \quad (7)$$

where ΔG_U(neutral), p, and Z are the free energy in the absence of electrostatic contribution, proportionality constant, and net charge, respectively. This equation is based on the classic and simplified model of Linderstrom-Lang, assuming that the charged groups were independent of each other and located with equal probability on the surface of the spherical protein molecule (*26*). This simplified equation is likely to be valid for the molten globule state because the electrostatic interactions are not site-specific in the molten globule state and the acetylated species are mixtures of various species with different sites of acetylation. The values of ΔG_U(neutral) and p were estimated to be 19.4 kJ/mol and 45 J/mol per square net charge, respectively (*26*). The dependence of ΔG_U on the degree of acetylation shows a saturating curve, indicating that the effects of acetylation decrease with the progression of acetylation. The fraction of the molten globule state calculated from ΔG_U reproduces the experiments: it cooperatively increases with degree of acetylation with a midpoint of three to four acetylations (Figure 4).

(ii) Exchange Rates of the Molten Globule State. Jeng et al. (*9*) studied the H/D exchange kinetics of the molten globule state of cytochrome *c* in 1.5 M NaCl at pD 2.2 and 20 °C. They analyzed the exchange kinetics with 2D H NMR and showed for the first time the structure of the molten globule state at the residue level: the three major helices in the native state and their common hydrophobic domain are largely preserved, while the loop region of the native structure is flexible and partly disordered. They estimated the protection factors, P, for 44 residues of the salt-stabilized molten globule state as well as those of the native state. The residues with P values higher than 500 were V11 (726), A15 (1120), M65 (507), L94 (619), I95 (2743), A96 (952), T97 (959), L98 (1935), and K99 (519), where the numbers in parentheses are the observed P values. The exchange rate of each amide proton in the molten globule state can be obtained by $k_{MG} = k_{int}/P(MG)$. For the residues not protected in the molten globule state, we use k_{int} of each residue.

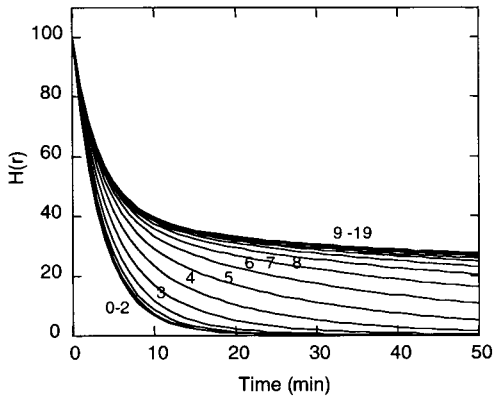

FIGURE 5: Simulated H/D exchange kinetics of cytochrome *c* in 18 mM DCl. The figures indicate the number of acetylated Lys residues.

Although the *P* values were likely to depend on the concentration of NaCl and pH, the reported values in 1.5 M NaCl at pD 2.2 were used for our simulation.

(iii) Exchange Rates of the Unfolded State. We can use the intrinsic exchange rates calculated with the amino acid sequence of horse cytochrome *c* according to Bai et al. (*28*), where the effects of only nearest-neighbor residues are considered. We neglected the effects of acetylation on k_{int}, and no correction was made.

Cytochrome *c* consists of 104 amino acids residues, containing 3 prolines, and the N-terminal is acetylated. For each of 99 amide protons, we simulated the exchange kinetics with the respective values of k_{int} and k_{MG} and with a common value of ΔG_U. Then, the kinetics of 99 amide protons were summed to obtain the overall exchange kinetics for each acetylated species. The kinetics of cytochrome *c* with different degrees of acetylation were then obtained by changing ΔG_U according to eq 5.

The simulated H/D exchange kinetics of various acetylated species (Figure 5) were similar to the observed kinetics. It is noted that we did not introduce any adjustment of the reported parameters in order to obtain the better fitting. It is amazing that the reported parameters reproduced the observed kinetics fairly well. Importantly, acetylation of up to three residues did not change the kinetics of the intact cytochrome *c*. Marked changes in the kinetic profile occurred between 4Ac-cyt *c* and 8Ac-cyt *c*. The simulated kinetics were independent of the extent of acetylation for the species with more than nine acetylated residues. To compare the observed and calculated kinetics quantitatively, we obtained the apparent time constant of the overall exchange reaction, when the number of remaining protected protons becomes 99/e (Figure 4). While it was 3.5 min for 0Ac-cyt *c*, it increased to 12.4 min for 13Ac-cyt *c*. Although the time constant for 13Ac-cytc was smaller than the observed value (27.8 min), the normalized transition curves were similar to each other, both showing a lag phase and increasing later than the conformational transition. These results indicate that the general two-process model of exchange (mechanism 4) and the parameters obtained from the literature are fairly valid for explaining the H/D exchange kinetics of cytochrome *c* in the molten globule state under various conditions of stability.

However, there were some differences between the observed and simulated kinetic curves. First, the amplitudes of observed proton occupancy were slightly higher than the calculated values. This was probably because of the contribution of exchangeable protons on the side chains. In addition, even for intact cytochrome *c*, the final level of the observed kinetics did not reach zero probably because of back-exchange during the measurements. Electrospray MS separated and distinguished coexisting compact molten globule molecules and disordered molecules on the basis of their net charges (Figure 1). The presence of only two clusters of charged states is consistent with a two-state mechanism of conformational transition. However, while the compact structure was detected even in 18 mM HCl (or DCl), highly acetylated 13Ac-cyt *c* still showed strong peaks of disordered conformation. These results were inconsistent with other observations including those of CD. As described before, this suggested that the distribution of two populations is altered when the protein molecule is subjected to electrospray ionization. We cannot exclude the possibility that this slightly affects our analysis of the exchange kinetics.

CONCLUSIONS

With electrospray MS, we systematically analyzed the H/D exchange kinetics of cytochrome *c* species with various degrees of acetylation and hence with various degrees of stability. MS enabled the simultaneous analysis of the variously acetylated species in the same solution, so that the separation of these species, as Goto and co-workers (*33*−35) did, was not necessary and the comparison of different species was exact. The acetylation of amino groups progressively retarded the exchange reaction, indicating the formation of the molten globule state protected from rapid exchange. However, the overall exchange kinetics were biased by the labile unfolded state, consistent with a two-process model of exchange under destabilized conditions. We simulated the exchange kinetics of acetylated species on the basis of the general two-process model and the parameters obtained from the literature (*9*, *34*, *36*). It is remarkable that, without any adjustment of the parameters for fitting, the simulated kinetics reproduced fairly well with the observed kinetics. This reasonable agreement indicates the validity of both the two-state transition model between the unfolded and molten globule states and the two-process model of H/D exchange. The two-process exchange model is thus important for understanding the structural dynamics of the intermediate state under conditions of marginal stability.

REFERENCES

1. Baldwin, R. L. (1993) *Curr. Opin. Struct. Biol. 3*, 84−91.
2. Kiefhaber, T., and Baldwin, R. L. (1995) *Biophys. Chem. 59*, 351−356.
3. Kiefhaber, T., and Baldwin, R. L. (1996) *Proc. Natl. Acad. Sci. U.S.A. 92*, 2657−2661.
4. Loh, S., Rohl, C., Kiefhaber, T., and Baldwin, R. L. (1996) *Proc. Natl. Acad. Sci. U.S.A. 93*, 1982−1987.
5. Li, R., and Woodward, C. (1999) *Protein Sci. 8*, 1571−1591.
6. Englander, S. W. (2000) *Annu. Rev. Biophys. Biomol. Struct. 29*, 213−238.
7. Udgaonkar, J. B., and Baldwin, R. L. (1988) *Nature 335*, 694−699.
8. Roder, H., Elöve, G. A., and Englander, S. W. (1988) *Nature 335*, 700−704.
9. Jeng, M.-F., Englander, S. W., EIöve, G. A., Wand, A. J., and Roder, H. (1990) *Biochemistry 29*, 10433−10437.

10. Hughson, F. M., Wright, P. E., and Baldwin, R. L. (1990) *Science 249*, 1544−1548.
11. Jennings, P. A., and Wright, P. E. (1993) *Science 262*, 892−896.
12. Sauder, J. M., and Roder, H. (1998) *Fold. Des. 3*, 293−301.
13. Suckau, D., Shi, Y., Beu, S. C., Senko, M. W., Quinn, J. P., Wampler, F. M., and McLafferty, F. W. (1993) *Proc. Natl. Acad. Sci. U.S.A. 90*, 790−793.
14. Katta, V., and Chait, B. T. (1993) *J. Am. Chem. Soc. 115*, 6317−6321.
15. Miranker, A., Robinson, C. V., Radford, S. E., Aplin, R. T., and Dobson, C. M. (1993) *Science 262*, 896−900.
16. Robinson, C. V., Grop, M., Eyles, S. J., Ewbank, J. J., Mayhew, M., Hartl, F. U., Dobson, C. M., and Radford, S. E. (1994) *Nature 372*, 646−651.
17. Wagner, D. S., and Anderegg, R. J. (1994) *Anal. Chem. 66*, 706−711.
18. Wang, F., and Tang, X.-J. (1996) *Biochemistry 35*, 4069−4078.
19. Chowdhury, S. K., Katta, V., and Chait, B. T. (1990) *J. Am. Chem. Soc. 112*, 9012−9013.
20. Feng, R., and Konishi, Y. (1992) *Anal. Chem. 64*, 2090−2095.
21. Ptitsyn, O. B. (1995) Molten globule and protein folding, *Adv. Protein Chem. 47*, 83−229.
22. Goto, Y., Takahashi, N., and Fink, A. L. (1990) *Biochemistry 29*, 3480−3488.
23. Hamada, D., Kidokoro, S., Fukada, H., Takahashi, K., and Goto, Y. (1994) *Proc. Natl. Acad. Sci. U.S.A. 91*, 10325−10329.
24. Kuroda, Y., Endo, S., Nagayama, K., and Wada, A. (1995) *J. Mol. Biol. 247*, 682−688.
25. Goto, Y., and Nishikiori, S. (1991) *J. Mol. Biol. 222*, 679−686.
26. Hagihara, Y., Tan, Y., and Goto, Y. (1994) *J. Mol. Biol. 237*, 336−348.
27. Kataoka, M., Hagihara, Y., Mihara, K., and Goto, Y. (1993) *J. Mol. Biol. 229*, 591−596.
28. Bai, Y. W., Milne, J. S., Mayne, L., and Englander, S. W. (1993) *Proteins: Struct., Funct., Genet. 17*, 75−86.
29. Lundblad, R. (1995) *Techniques in Protein Modification*, p 132, CRC Press, Boca Raton, Ann Arbor, London, and Tokyo.
30. Ramanathen, R., Gross, M. L., Zielinski, W. L., and Layloff, T. P. (1997) *Anal. Chem. 69*, 5142−5145.
31. Glockner, M. O., Borchers, C., Fiedler, W., Suckau, D., and Przybylski, M. (1994) *Bioconjugate Chem. 5*, 583−590.
32. Scholtz, J. M., and Baldwin, R. L. (1993) *Biochemistry 32*, 4604−4608.
33. Johnson, R. S., and Walsh, K. A. (1994) *Protein Sci. 3*, 2411−2418.
34. Goto, Y., Hagihara, Y., Hamada, D., Hoshino, M., and Nishii, I. (1993) *Biochemistry 32*, 11878−11885.
35. Hvidt, A, and Nielsen, S. O. (1966) *Adv. Protein Chem. 21*, 288−386.
36. Woodward, C., Simon, I., and Tüchsen, E. (1982) *Mol. Cell. Biochem. 48*, 135−160.
37. Kim, K.-S., and Woodward, C. (1993) *Biochemistry 32*, 9609−9613.
38. Mayo, S. L., and Baldwin, R. L. (1993) *Science 262*, 873−876.
39. Qian, H., Mayo, S. L., and Morton, A. (1994) *Biochemistry 33*, 8167−8171.
40. Bai, Y., Milne, J. S., Mayne, L., and Englander, S. W. (1994) *Proteins 20*, 4−14.
41. Bai, Y., Sosnick, T. R., Mayne, L., and Englander, S. W. (1995) *Science 269*, 192−197.
42. Milne, J. S., Xu, Y., Mayne, L. C., and Englander, S. W. (1999) *J. Mol. Biol. 290*, 811−822.

BI002762C